Volume 9 | Number 28 | 28 July 2018 | Pages 6009–6158

Chemical Science

rsc.li/chemical-science

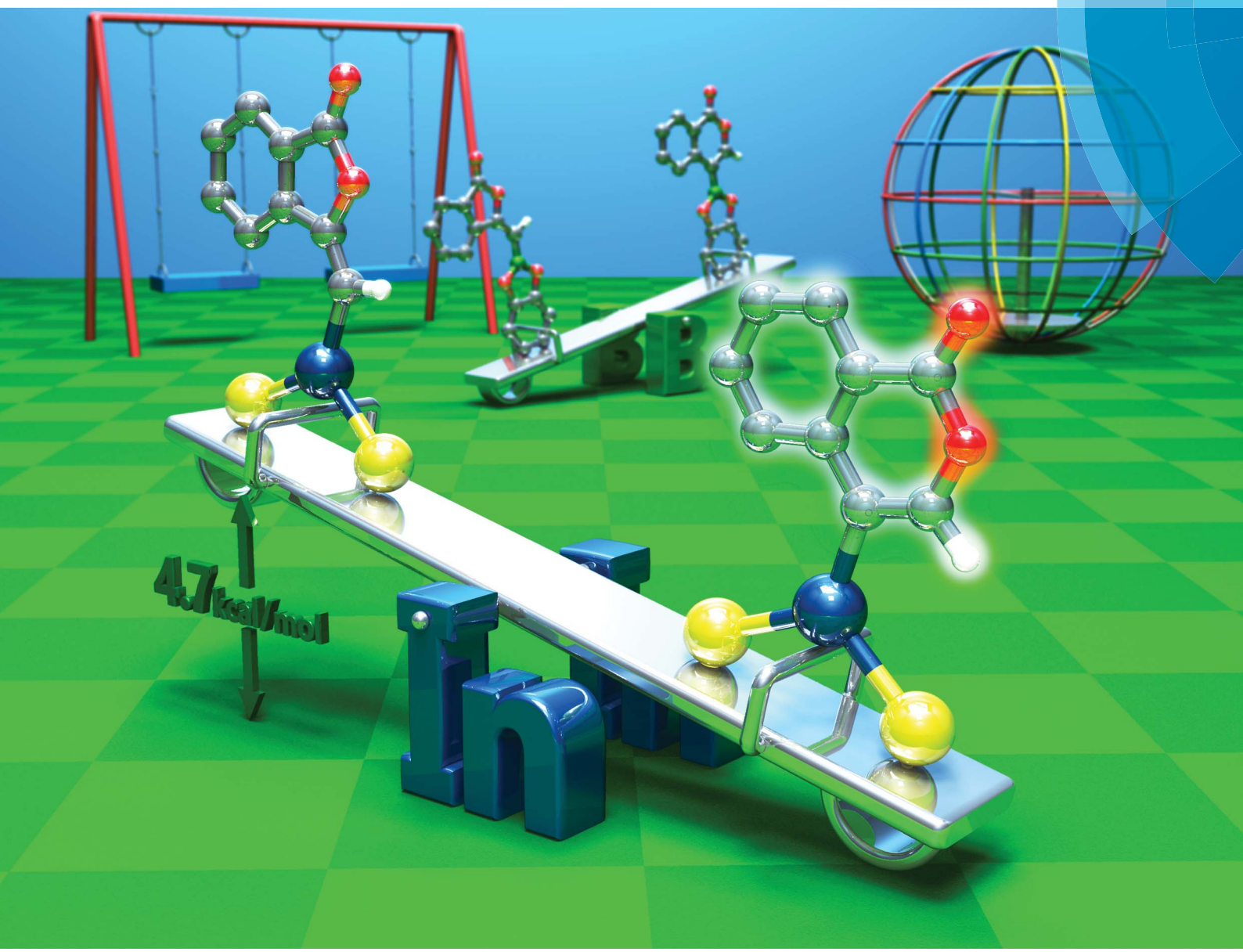

ISSN 2041-6539

ROYAL SOCIETY OF CHEMISTRY

EDGE ARTICLE

Yoshihiro Nishimoto, Makoto Yasuda *et al.*

Selective oxymetalation of terminal alkynes *via* 6-*endo* cyclization: mechanistic investigation and application to the efficient synthesis of 4-substituted isocoumarins

Chemical Science

EDGE ARTICLE

View Article Online
View Journal | View Issue

Cite this: *Chem. Sci.*, 2018, **9**, 6041

Selective oxymetalation of terminal alkynes *via* 6-*endo* cyclization: mechanistic investigation and application to the efficient synthesis of 4-substituted isocoumarins†

Yuji Kita, [a] Tetsuji Yata, [a] Yoshihiro Nishimoto, *[b] Kouji Chiba[c] and Makoto Yasuda *[a]

The cyclization of heteroatom-containing alkynes with π acidic metal salts is an attractive method to prepare heterocycles because the starting materials are readily available and the organometallic compounds are useful synthetic intermediates. A new organometallic species in the heterocyclization provides an opportunity to synthesize heterocycles that are difficult to obtain. Herein, we describe a novel cyclic oxymetalation of 2-alkynylbenzoate with indium or gallium salts that proceeds with an unusual regioselectivity to give isocoumarins bearing a carbon–metal bond at the 4-position. This new type of metalated isocoumarin provided 3-unsubstituted isocoumarins that have seldom been investigated despite their important pharmacological properties. Indium and gallium salts showed high performance in the selective 6-*endo* cyclization of terminal alkynes while boron or other metals such as Al, Au, and Ag caused 5-*exo* cyclization or decomposition of terminal alkynes, respectively. The metalated isocoumarin and its reaction intermediate were unambiguously identified by X-ray crystallographic analysis. The theoretical calculation of potential energy profiles showed that oxyindation could proceed *via* 6-*endo* cyclization under thermodynamic control while previously reported oxyboration would give a 5-membered ring under kinetic control. The investigation of electrostatic potential maps suggested that the differences in the atomic characters of indium, boron and their ligands would contribute to such a regioselective switch. The metalated isocoumarins were applied to organic synthetic reactions. The halogenation of metalated isocoumarins proceeded to afford 4-halogenated isocoumarins bearing various functional groups. The palladium-catalyzed cross coupling of organometallic species with organic halides gave various 4-substituted isocoumarins. A formal total synthesis of oosponol, which exhibits strong antifungal activity, was accomplished.

Received 4th April 2018
Accepted 13th June 2018

DOI: 10.1039/c8sc01537f

rsc.li/chemical-science

Introduction

Heterocyclic compounds have attracted much attention in pharmaceutical chemistry as well as in photochemistry and also play a pivotal role as building blocks in organic synthetic transformation.[1] Therefore, a novel efficient synthetic method for heterocyclic frameworks is highly desired in various fields of chemistry. Many well-established methods are available in the literature.[2] The heterocyclization of ω-heteroatom-substituted alkynes using π acidic metal salts is undoubtedly a powerful strategy for the preparation of heterocycles (Scheme 1).[3] This addition reaction uses readily available alkynes as a starting material. Furthermore, metal salt-mediated cyclization spontaneously forms a carbon–metal bond and a heterocyclic framework and produces organometallic intermediates leading to target heterocycles *via* appropriate synthetic reactions such as cross coupling. These features allowed us to directly access various substituted heterocycles from simple organic substrates.

Various heteroatom-containing alkynes have been investigated for use in the synthesis of heterocyclic compounds using π acidic metal salts. Alkyne **A** includes a carbonyl moiety and is a feasible and beneficial substrate to obtain 5- or 6-membered oxacyclic alkenylmetals (Scheme 2A). When **A** is treated with a metal salt (MX), oxymetalation proceeds to afford heterocyclic

[a]*Department of Applied Chemistry, Graduate School of Engineering, Osaka University, 2-1 Yamadaoka, Suita, Osaka 565-0871, Japan. E-mail: yasuda@chem.eng.osaka-u.ac.jp*

[b]*Frontier Research Base for Global Young Researchers Center for Open Innovation Research and Education (COiRE), Graduate School of Engineering, Osaka University, 2-1 Yamadaoka, Suita, Osaka 565-0871, Japan. E-mail: nishimoto@chem.eng.osaka-u.ac.jp*

[c]*Material Science Division, MOLSIS Inc., 1-28-38 Shinkawa, Chuo-ku, Tokyo 104-0033, Japan*

† Electronic supplementary information (ESI) available: Additional experimental data, characterization, calculation data and experimental details. CCDC 1576342–1576344 and 1579824. For ESI and crystallographic data in CIF or other electronic format see DOI: 10.1039/c8sc01537f

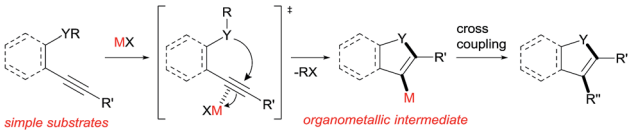

Scheme 1 Metal salt-mediated heterocyclization of ω-heteroatom-substituted alkynes.

compounds through either 5-*exo* or 6-*endo* cyclization (Type *exo* or *endo*). Considering that the structure of **A** bears either an internal (R = alkyl, aryl, *etc.*) or a terminal alkyne (R = H), oxymetalation can be distinguished by four types of reaction courses: Type *exo*-i, Type *exo*-t, Type *endo*-i, and Type *endo*-t. In Types *exo*-i and *exo*-t, the furan frameworks **B** and **C** have a metal carbenoid moiety and are obtained *via* the isomerization of zwitterion intermediates.[4,5] On the other hand, Types *endo*-i and *endo*-t lead to 1*H*-isochromen derivatives **D** and **E** *via* the elimination of R′X from zwitterion intermediates.[6,7] Among these four types, only Type *endo*-t is kinetically unfavorable due to an unstable cationic transition state *via* an anti-Markovnikov addition manner (Scheme 2B). Furthermore, recent theoretical research about the regioselectivity of cyclization revealed that the nucleophilic cyclization of alkynes displays *exo* selectivity intrinsically.[8] On the other hand, Lewis acidic metals can promote *endo* cyclization by decrease of the stereoelectronic penalty, but the *exo* cyclization was not disturbed, and, thus, the cyclization showed low selectivity.[7,9] For the above reasons, there is no report of a preparation method for species **E** *via* Type *endo*-t in contrast to the cases of Types *exo*-i, *exo*-t, and *endo*-i, for which target organometallic compounds (**B–D**) are well established.[4b,5a,6c,6e] If the reaction course of oxymetalation is realized from **A** to **E** in Type *endo*-t,[10] various 6-membered heterocycles based on **E**, which have been difficult to obtain and remain unknown, should be synthesized. Therefore, the establishment of a strategy for Type *endo*-t is an important challenge in heterocyclic chemistry.

Isocoumarins are an important class of oxygen-containing heterocycles that exhibit a wide range of pharmacological properties.[11] Thus, the development of their general synthetic method has attracted much attention. The reaction of Type *endo* would be a powerful tool for the synthesis of isocoumarins (Scheme 3A). In fact, reports have described the oxymetalation of 2-alkynylbenzoate **1** (R = alkyl, alkenyl, aryl) for Type *endo*-i and application to the synthesis of isocoumarins.[6a,6b,6e] Recently, Blum reported an excellent method for the construction of 4-borylated isocoumarins by the oxyboration of the internal alkynes **1** in the Type *endo*-i reaction course (Scheme 3B).[6e] However, terminal alkyne **1** (R = H) gave only a 5-*exo* cyclization product according to the Markovnikov rule (blue path in Scheme 3C).[6e] This result prompted us to explore the oxymetalation of the terminal alkynes **1** for Type *endo*-t. The oxymetalation of Type *endo*-t provides 3-unsubstituted and 4-substituted isocoumarins that are seldom investigated due to the lack of synthetic methods,[12] and limited substituents have been introduced at the 4-position despite the well-known beneficial significant bioactivity characteristics such as antitumor,[13] antiangiogenic,[14] antifungal,[15] and antibiotic.[16]

Our group developed the indium or gallium salt-mediated carbometalation of simple terminal alkynes with silyl ketene acetals by utilizing their high π electron affinity and moderate Lewis acidity.[17] In this context, we investigated the Type *endo*-t reaction of 2-ethynylbenzoate using indium or gallium trihalides for the synthesis of corresponding metalated isocoumarins. In this report, we successfully achieved a 6-*endo* selective oxymetalation of terminal alkynes and fully characterized the target organometallic species **E1** *via* an NMR study and X-ray crystallographic analysis. Furthermore, the intermediate **F1** was isolated, which revealed that oxymetalation proceeds *via* the zwitterion intermediate **F1**, and the elimination

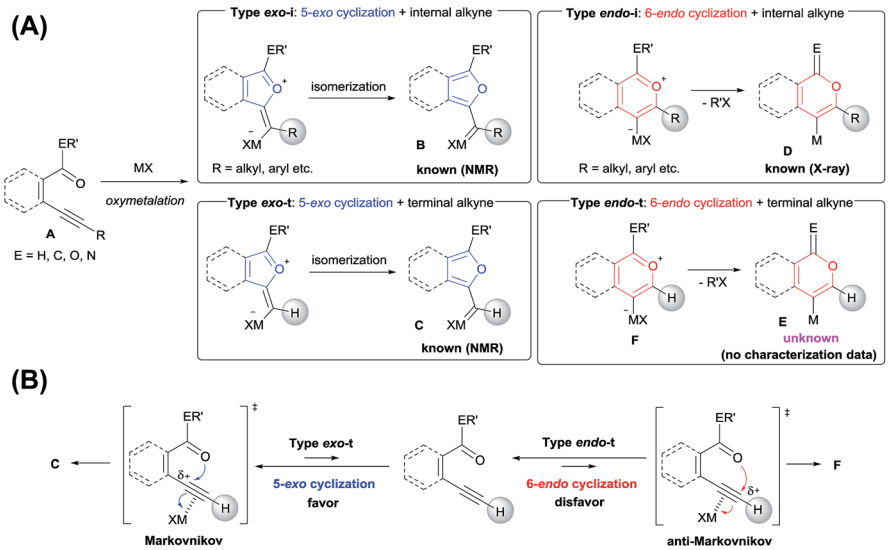

Scheme 2 (A) Four types of metalated heterocycles from the oxymetalation of alkyne **A** including a carbonyl moiety. (B) Comparison of the transition states of Type *exo*-t with Type *endo*-t.

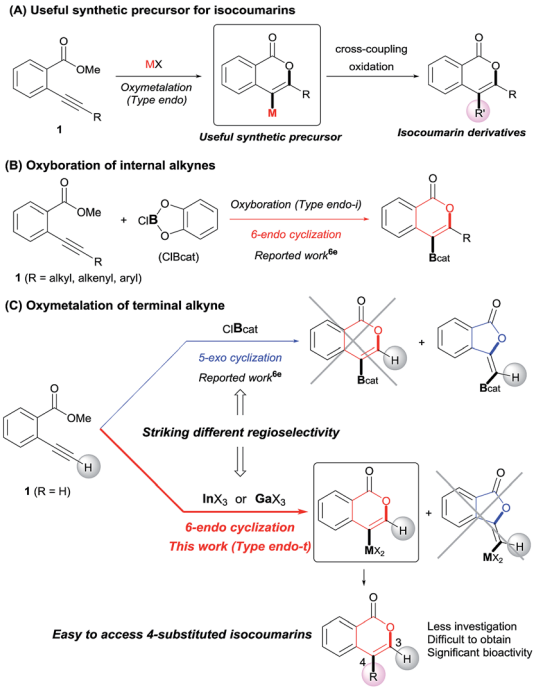

Scheme 3 (A) Oxymetalation of 2-alkynylbenzoate **1** followed by transformation for the construction of isocoumarins. (B) Previously reported oxyboration of internal alkynes to generate 4-borylated isocoumarins. (C) Oxymetalation of terminal alkynes, reported oxyboration for 5-membered compounds (blue path), and our developed oxymetalation for 6-membered compounds (red path).

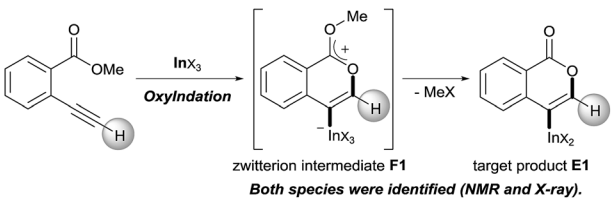

Scheme 4 Oxyindation of alkynes for the synthesis of an isocoumarin framework *via* a zwitterion intermediate.

Table 1 Effect of Lewis acids on the oxymetalation of 2-ethynylbenzoate **1a**[a]

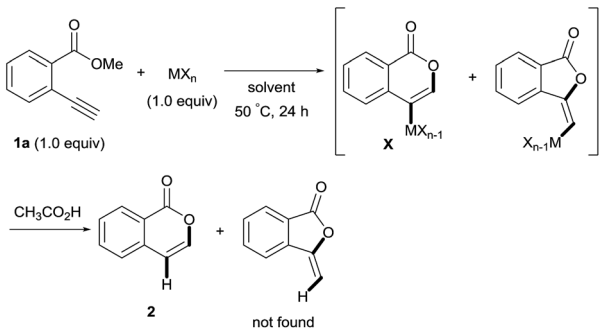

Entry	MX_n	Solvent	Yield[b] of **2** (%)
1	$InCl_3$	Toluene	13
2[c]	$InBr_3$	Toluene	82 (77% D)
3[c]	InI_3	Toluene	79 (91% D)
4	$GaBr_3$	Toluene	30
5	GaI_3	Toluene	77
6	$AlCl_3$	Toluene	0
7	AlI_3	Toluene	0
8	BBr_3	Toluene	0
9	$TiCl_4$	Toluene	0
10	$PdCl_2$	Toluene	0
11	$CuBr_2$	Toluene	0
12	$FeBr_3$	Toluene	0
13	$AuCl_3$	Toluene	7
14	AuCl	Toluene	5
15	AgOTf	Toluene	31
16	AuCl/AgOTf	Toluene	18
17[d]	InI_3	Toluene	61
18	InI_3	$ClCH_2CH_2Cl$	78
19	InI_3	ClC_6H_5	57
20	InI_3	Hexane	57
21	InI_3	CH_3CN	17
22	InI_3	THF	0

[a] Reaction conditions: **1a** (0.5 mmol), Lewis acid MX_n (0.5 mmol), solvent (1 mL), 50 °C, 24 h. [b] The yield of **2** was determined by ^1H NMR. [c] The reaction mixture was quenched with CH_3CO_2D (30 equiv., 5 min) and a subsequent addition of H_2O (10 mL). [d] 35 °C.

of the alkyl halide gives the target product **E1** (Scheme 4). While benzopyrylium species such as **F** are known as highly reactive intermediates in the proposed catalytic oxymetalation cycle,[10a,18] the isolation of species **F** is a challenging issue.[10e,10f,19] To the best of our knowledge, **F1** is the first example of a fully characterized benzopyrylium intermediate **F**. In addition, we fully disclosed the mechanism by combining experimental data and theoretical calculation. These mechanistic investigations were consistent with the achievement of isolation of the zwitterion intermediate and demonstrated that its stability is a crucial point in this remarkable cyclization regioselectivity.

Results and discussion

Optimization of reaction conditions

First, we examined the effect of Lewis acids on oxymetalation using methyl 2-ethynylbenzoate **1a** (Table 1). The reaction of **1a** with metal halides was carried out in toluene at 50 °C, and the reaction mixture was quenched with acetic acid. The reaction using $InCl_3$ afforded the target isocoumarin **2** *via* 6-*endo* cyclization, albeit in a low yield (entry 1). Gratifyingly, $InBr_3$ and InI_3 mediated oxymetalation smoothly proceeded in a 6-*endo* cyclization fashion to give **2** in high yields (entries 2 and 3). In these cases, the reaction mixture was quenched with deuterated acetic acid to afford **2** bearing deuterium at the 4-position. We did not observe an isocoumarin bearing deuterium at the 3-position which could be produced through the generation of indium acetylide[20] followed by Lewis acid mediated cycloaddition. The reaction using InI_3 showed a higher ratio of D/H than the case of $InBr_3$. This result suggested the more efficient generation of the alkenylmetal intermediate **X** in the case of InI_3. Gallium salts were also suitable for the 6-*endo* cyclization of **1a**, and GaI_3 gave a high yield (entries 4 and 5). On the other hand, typical Lewis acids such as $AlCl_3$, AlI_3, BBr_3 and $TiCl_4$ were

ineffective (entries 6–9). Transition metal salts such as $PdCl_2$, $CuBr_2$ and $FeBr_3$ provided no target product and resulted in a decomposition of **1a** (entries 10–12). Alkynophilic π-acids such as gold and silver salts were subjected to the present cyclization. It was found that $AuCl_3$, AuCl, AgOTf and AuCl/AgOTf resulted in low yields (entries 13–16). A decrease in yield was observed at lower temperature (entry 17). The solvent effect was examined on oxyindation using InI_3. Dichloroethane as a solvent provided a good yield while chlorobenzene and hexane afforded only moderate yields (entries 18–20). The yields were appreciably decreased in CH_3CN and THF (entries 21 and 22) probably because the coordination of these solvents to InI_3 decreased the Lewis acidity. Finally, InI_3 was the most effective Lewis acid, and, therefore, we chose entry 3 to represent the optimal conditions.

Mechanistic investigation

To gain insight into the reaction mechanism, we used ^{1}H NMR spectroscopy to monitor the oxyindation. When 2-alkynylbenzoate **1a** was mixed with InI_3 in $CDCl_3$ at −30 °C, no reaction occurred. At −5 °C, some amount of a new product was observed (see Fig. S1 and S2† in the ESI). At room temperature, a large amount of white precipitation was formed. This white solid was also obtained in the reaction of **1a** with InI_3 in toluene at room temperature (eqn (1)). X-ray crystallographic analysis revealed that the white solid was a 6-membered oxacyclic zwitterion **3** bearing a carbon–indium bond (Fig. 1). The bond lengths of the two carbon–oxygen bonds (C1–O1 = 1.267 Å and C1–O2 = 1.298 Å) in the zwitterion **3** existed between a C–O double bond (1.203 Å) and the single bond (1.377 Å) of a typical isocoumarin derivative,[21] and, thus, the positive charge was delocalized in an ester moiety. The indium atom was coordinated to three iodines and showed a distorted tetrahedral structure with a formal negative charge. The formed zwitterionic alkenyl indium **3** was heated at 50 °C in toluene to give a neutral alkenylindium product **4a**, quantitatively by the elimination of MeI (eqn (2)). Although a suitable single crystal of **4a** for X-ray analysis was not obtained, we successfully conducted X-ray diffraction analysis of nitro-substituted alkenylindium **4b** produced from 2-ethynyl-5-nitrobenzoate **1b** (eqn (3) and Fig. 2). The bond lengths of C1–O1 (1.211 Å) and C1–O2 (1.367 Å) were similar to those of a reported isocoumarin framework.[21] The indium complex **4b** displayed trigonal bipyramidal coordination with two THF ligands in axial positions. These results indicated a two-step pathway including a fast cyclization and a slow elimination of MeI during the 6-*endo* oxyindation process from **1** to **4**.

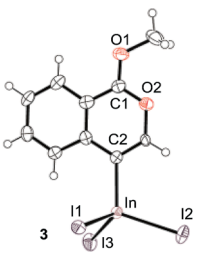

Fig. 1 The X-ray crystallographic structure of zwitterion intermediate **3** with the thermal ellipsoids shown at 50% probability (CCDC 1579824). Selected bond lengths (Å): C1–O1 = 1.267(9), C1–O2 = 1.298(11), C2–In = 2.171(7), In–I1 = 2.7392(8), In–I2 = 2.7219(8), and In–I3 = 2.6915(7).

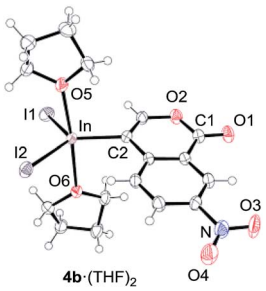

Fig. 2 The X-ray crystallographic structure of an isocoumarin including a carbon–indium bond at the 4-position, **4b**·$(THF)_2$, with the thermal ellipsoids shown at 50% probability (CCDC 1576342). Selected bond lengths (Å) and angles (deg): C1–O1 = 1.211(4), C1–O2 = 1.367(5), C2–In = 2.162(3), In–I1 = 2.7148(4), In–I2 = 2.7005(4), In–O5 = 2.318(3), In–O6 = 2.371(3), O5–In–O6 = 175.44(10), I1–In–C2 = 116.70(11), C2–In–I2 = 125.51(11), and I2–In–I1 = 117.621(12).

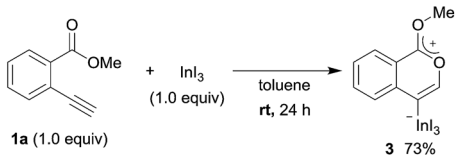

(1)

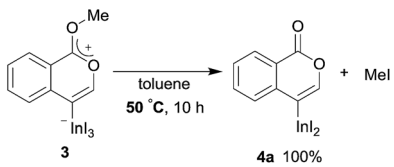

(2)

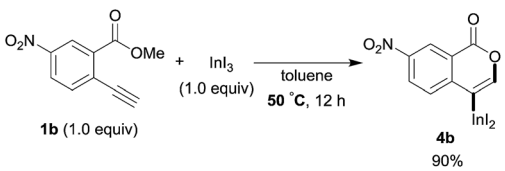

(3)

Theoretical calculation for oxyindation

A mechanism for the formation of the target isocoumarin **4a** using InI_3 is proposed in Scheme 5, wherein InI_3 is coordinated to the alkyne moiety in **5**, oxyindation proceeds *via* 6-*endo* cyclization to give the zwitterion intermediate **3**, and, finally, the elimination of MeI affords **4a**.

Density functional theory (DFT) calculations were performed to more thoroughly consider the reaction mechanism. The calculation of the potential energy profile for 6-*endo* cyclization

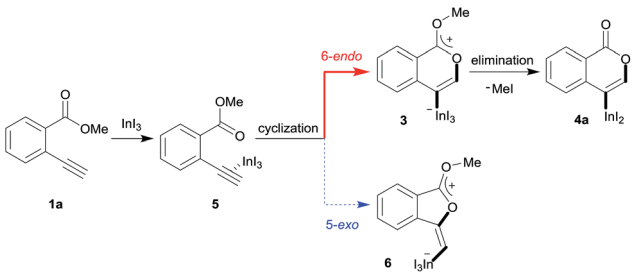

Scheme 5 A proposed mechanism for the formation of the isocoumarin **4a**.

(red) is shown in Fig. 3. We selected **1a** and In_2I_6 as the starting materials because InI_3 exists in a dimer fashion.[22] The coordination of two **1a** to In_2I_6 dissociates the aggregation of InI_3 to give complex **7**, in which InI_3 is chelated with the alkyne moiety and carbonyl group of **1a** (Fig. S3† in the ESI shows the detailed mechanism of generating the complex **7** from **1a** and In_2I_6). The dissociation of the carbonyl oxygen atom generates complex **5**, in which InI_3 directly activates the alkyne moiety. In this pathway, the anti-addition of InI_3 and the ester moiety to the alkyne moiety proceeds in a concerted mechanism to provide a stable 6-membered zwitterion intermediate **3**. The elimination of MeI proceeds in an intermolecular fashion, because the intramolecular elimination of MeI requires a very unstable intermediate (Fig. S4† in the ESI shows the potential energy profile for the intramolecular elimination of MeI). Two zwitterions aggregate in a head-to-tail fashion to give complex **8**, and then the elimination step starts from **8**. The intermolecular nucleophilic substitution of the methyl group by I^- proceeds in an S_N2-mechanism to give complex **10** and MeI, and then a subsequent elimination of MeI affords the target product **4a**.[23] A carbonyl group of **4a** coordinates to the indium atom of another **4a** to give the stable dimeric product **13**. The activation energy of the elimination step (**8** to TS2-6-*endo*, 28.7 kcal mol^{-1})

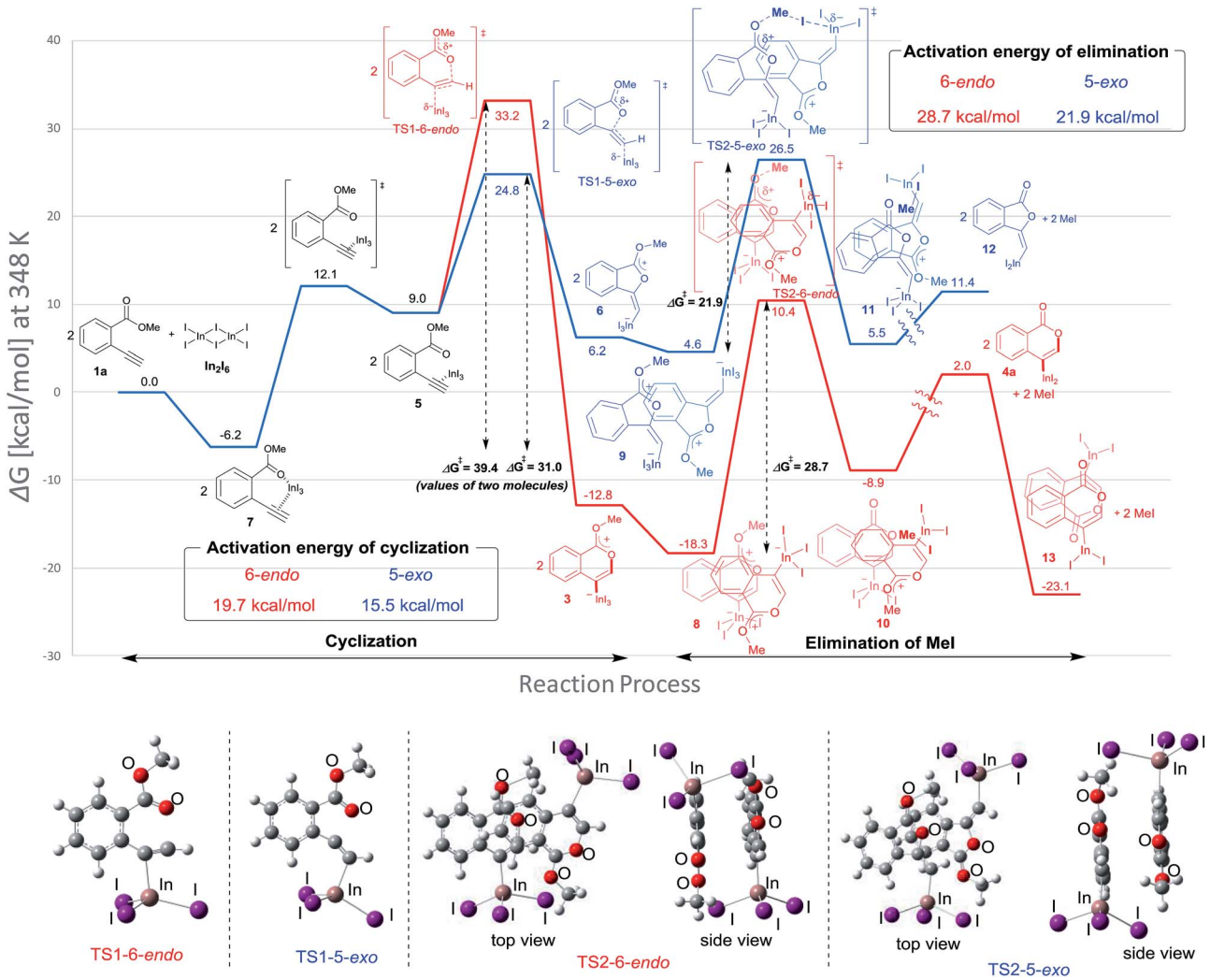

Fig. 3 The energy profiles of 6-*endo* and 5-*exo* oxyindations and 3D molecular structures of transition states. DFT calculation was performed using wB97XD/6-31+G (d,p) for C, H, and O and using DGDZVP for In and I. Solvation effect was introduced using the IEFPCM model, and toluene was used as a solvent.

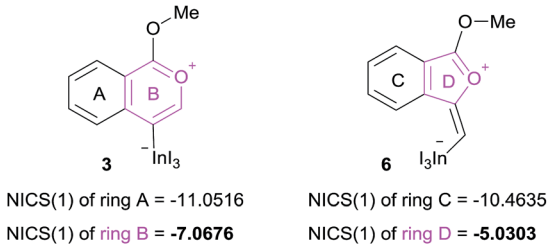

Fig. 4 NICS(1) values of 6-membered zwitterion **3** and 5-membered zwitterion **6**. The aromaticity was calculated using B3LYP/6-31G (d,p) for C, H, and O and using DGDZVP for In and I for their optimized structures.

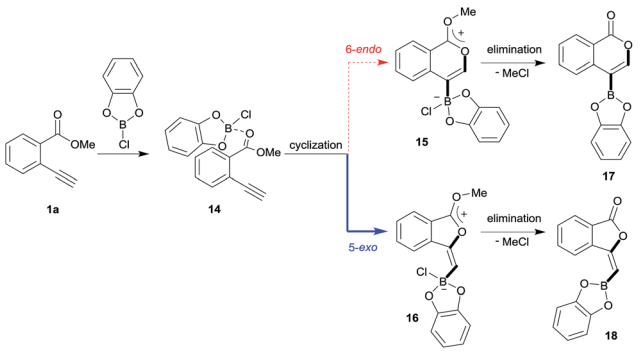

Scheme 6 A proposed mechanism for oxyboration.

is much higher than that of the cyclization step (7 to TS1-6-*endo*, 19.7 kcal mol^{-1}).[24] Therefore, the elimination of MeI is a rate-determining step. We also calculated the 5-*exo* cyclization pathway (blue) to investigate the regioselectivity. This process proceeds *via* concerted cyclization, wherein the 5-membered zwitterion **6** is much more unstable than the 6-membered version **3**. The intermolecular elimination of MeI takes place in an S_N2-manner (**9** to **11**). The transition state (TS2-5-*exo*) shows the highest energy level, and it is even higher than the energy profile of the 6-*endo* cyclization process (red) due to the instability of the 5-membered zwitterion **6**.

In order to clarify the unique 6-*endo* cyclization selectivity of oxyindation, the energy profiles of the two cyclization manners were compared. The activation energy of 5-*exo* cyclization is lower (**7** to TS1-5-*exo*, 15.5 kcal mol^{-1}) than that of 6-*endo* cyclization (**7** to TS1-6-*endo*, 19.7 kcal mol^{-1}). However, 5-*exo* cyclization is reversible because the activation energy for the elimination of MeI (**9** to TS2-5-*exo*, 21.9 kcal mol^{-1}) is much higher than that of retro-cyclization (**6** to TS1-5-*exo*, 9.3 kcal mol^{-1}) due to the instability of the zwitterion **6**. On the other hand, during 6-*endo* cyclization, both activation energies of elimination (**8** to TS2-6-*endo*, 28.7 kcal mol^{-1}) and retro-cyclization (**3** to TS1-6-*endo*, 23.0 kcal mol^{-1}) are high because the 6-membered zwitterion intermediate **3** is thermodynamically stable. This result indicates that 6-*endo* cyclization is irreversible and the most thermodynamically stable form of intermediate **8** is exclusively generated to provide the target product **4a**, which is consistent with the successful isolation of the zwitterion intermediate **3** (Fig. 1). Therefore, oxyindation proceeds under thermodynamic control to afford the stable 6-membered product **4a**. We also calculated an energy profile of $InCl_3$-mediated oxyindation and found the same pathway with the case of InI_3 (see Fig. S5† in the ESI). The activation energy of the elimination step in the case of $InCl_3$ is higher than that of InI_3 because of the low nucleophilicity of Cl^-, and it caused much less reactivity of $InCl_3$ (entry 1, Table 1).

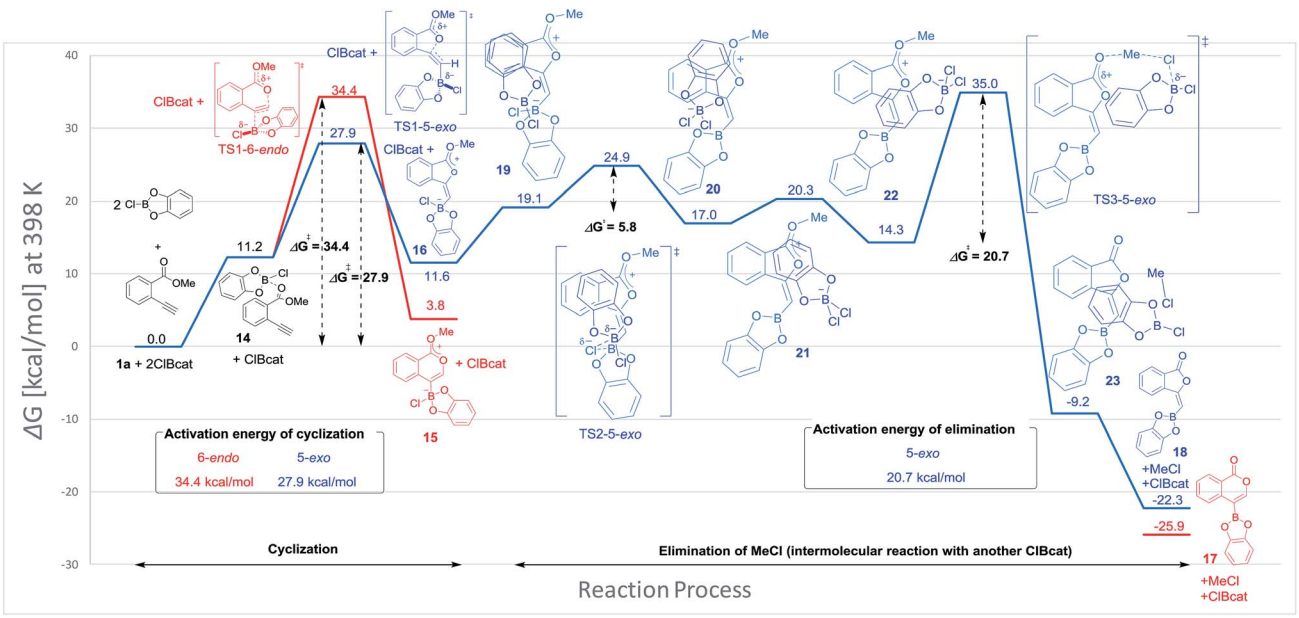

Fig. 5 The energy profiles of 5-*exo* and 6-*endo* oxyborations. DFT calculation was performed with wB97XD/6-31+G (d,p) for C, H, O, B, and Cl. Solvation effect was introduced using the IEFPCM model, and toluene was used as a solvent.

The remarkable regioselectivity of oxyindation is ascribed to the differences in stability between the 6-membered zwitterion **3** and the 5-membered **6**. Zwitterion **3** is much more stable than **6**, and this difference in stability originates from the aromaticity of these compounds, although ring strain is also a consideration. To verify this possibility, the aromaticity of zwitterions was evaluated *via* NICS(1)[25] (Fig. 4), and the 6-membered compound **3** showed a higher level of aromaticity than **6**.

Theoretical calculation for oxyboration

Blum and co-workers reported that the oxyboration of **1a** using B-chlorocatecholborane (ClBcat) gave a 5-membered product[6e] rather than the 6-membered version (Scheme 6). ClBcat is coordinated to the carbonyl moiety of **1a**. Then, oxyboration proceeds *via* 5-*exo* cyclization to give the zwitterion intermediate **16**, and the elimination of MeCl gives the target product **18**. We also performed DFT calculation of oxyboration to investigate the striking change in the regioselectivity between oxyboration and oxyindation. First, the calculation of oxyboration was performed for a similar oxyindation mechanism *via* concerted cyclization and S_N2-type elimination of MeCl from aggregated zwitterion intermediates (see Fig. S6† in the ESI). We considered another possibility for the elimination step, because the recent theoretical investigation of ClBcat-mediated heterocyclization has shown other mechanisms,[26] whereby the Me group is attacked either by dissociated chloride[26a] or by $[Cl_2Bcat]^-$.[26b] Thus, we considered these additional two plausible elimination steps assisted by either free Cl^- or $[Cl_2Bcat]^-$ (see Fig. S7† in the ESI and Fig. 5 and 6). The result of comparison between these three pathways showed that the most probable path was the use of $[Cl_2Bcat]^-$ (details of the comparison are shown in the ESI†).

The total reaction profile of oxyboration is described in Fig. 5 and 6. In that profile, 5-*exo* cyclization from **1a** and 2ClBcat to **16** has an activation energy (27.9 kcal mol^{-1}) that is lower than that of 6-*endo* cyclization (**1a** and 2ClBcat to **15**, 34.4 kcal mol^{-1}). The chloride moiety of zwitterion **16** coordinates to another ClBcat to provide complex **19**. The chloride transfer process (**19** to **20**) has a low energy barrier (5.8 kcal mol^{-1}), and $[Cl_2Bcat]^-$ is generated rapidly. Cl in $[Cl_2Bcat]^-$ approaches the methyl group in the ester moiety (**20** → **21** → **22**), and an elimination of MeCl (**22** to **23**) in the S_N2-mechanism occurs to give 5-membered product **18**. The activation energy of the elimination of MeCl (**22** to TS3-5-*exo*) is 20.7 kcal mol^{-1}, which allows the elimination of MeCl to proceed smoothly to give the final product **18**. The fast elimination step allows oxyboration to proceed under kinetic control to accomplish the 5-*exo* selective cyclization.

Comparing the transition state of the cyclization step in oxyindation with that in oxyboration based on an electrostatic potential map.

The significant difference between oxyindation and oxyboration was investigated because each showed a characteristic energy profile, particularly for the cyclization step. The energy barrier of cyclization in oxyindation (6-*endo*: 19.7 kcal mol^{-1}, 5-*exo*: 15.5 kcal mol^{-1}) is much lower than that of oxyboration (6-*endo*: 34.4 kcal mol^{-1}, 5-*exo*: 27.9 kcal mol^{-1}). Therefore, the electrostatic potential maps for the transition states of cyclization (TS1-6-*endo* and TS1-5-*exo*) were calculated (Fig. 7). The value of V_{min}, which represents the most negative surface electrostatic potential, was investigated to evaluate the degree of localization for a negative charge.[27] The V_{min} of the organoindium species (left, in Fig. 7) was less negative than that of boron (right, in Fig. 7), which showed that the negative charge was delocalized in the transition state of oxyindation compared with oxyboration. The value of V_{max}, which is the most positive surface electrostatic potential, was also calculated and was less affected by the differences in the metals (see Table S2† in the ESI). The polarizability of the indium, boron and heteroatoms binding to

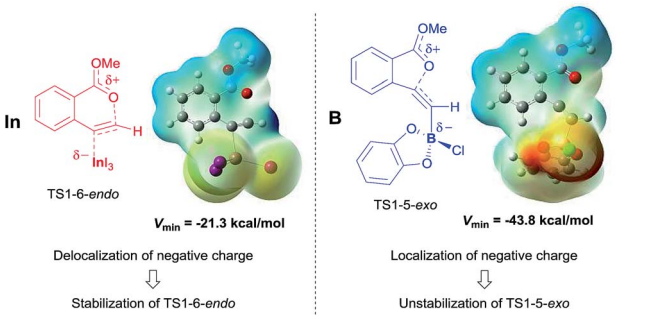

Fig. 7 Electrostatic potential maps were calculated on the 0.001 au isosurface of electron density for optimized structures of the transition states of oxyindation (left) and oxyboration (right). The potential is depicted by a color gradient from the most negative (red) to the most positive (blue) value (kcal mol^{-1}). V_{min} represents the most negative surface electrostatic potential.

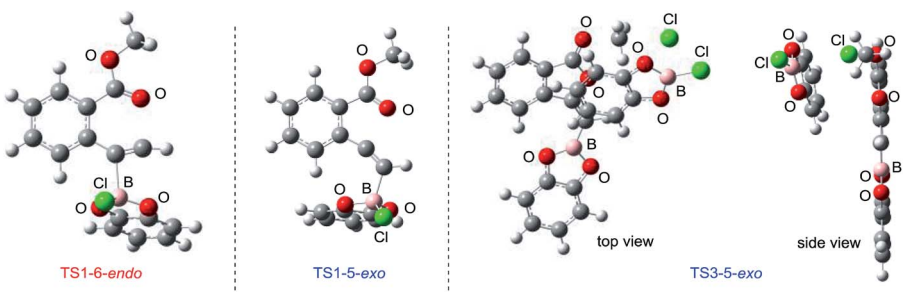

Fig. 6 3D molecular structures of transition states in oxyborations.

a metal explained these results. Indium and iodine atoms have large polarizability (α_{In} = 69 a.u. and α_I = 35.1 a.u.),[28] and the increasing negative charge in the TS1 of oxyindation was efficiently delocalized to stabilize the zwitterionic TS1-6-*endo*.[29] On the other hand, boron, chlorine and oxygen atoms have smaller polarizability (α_B = 20.5 a.u., α_{Cl} = 14.7 a.u., and α_O = 6.04 a.u.)[28] than indium and iodine atoms, so that TS1-5-*exo* becomes unstable due to the localization of a negative charge. The difference in the fundamental features between indium and boron atoms imparts a significant amount of influence on the regioselectivity of oxymetalation.

Summary of DFT calculation

In oxyindation (Fig. 8A), the activation energy of 5-*exo* cyclization is much lower than that required for the elimination of MeI to lead to reversible 5-*exo* cyclization. Therefore, the thermodynamically stable 6-membered zwitterion **3** was selectively produced to accomplish the remarkable 6-*endo* selectivity. The elimination step from **3** is a rate-determining step that provides the target metalated isocoumarin **4a**. On the other hand, the energy barrier for cyclization in oxyboration (Fig. 8B) is higher than that for the elimination of MeCl and the cyclization step is a rate-determining step, which leads to irreversible 5-*exo* cyclization to afford the 5-membered product **18** under kinetic control. Therefore, the activation energies of cyclization as well as elimination are important factors to determine the regioselectivity in cyclization.

Application to the synthesis of isocoumarin derivatives

Our developed oxyindation was applied to the synthesis of isocoumarin derivatives. First, the gram-scale synthesis of an organoindium species was carried out. Methyl ester **1a** (10 mmol) reacted with InI_3 to give organoindium **4a**, and 1.14 g of isocoumarin was isolated by the addition of H_2O (Scheme 7).

Next, the oxidation of the produced alkenylindium compounds was performed (Table 2). An oxyindation of **1a** using InI_3 was carried out, and the organoindium **4a** was oxidized with $PhI(OAc)_2$ in a one-pot procedure to give 4-iodoisocoumarin **24a** (entry 1). Subjecting $InBr_3$ to the oxidation reaction provided 4-bromoisocoumarin **25a** in a high yield (entry 2). Therefore, various types of 2-alkynylbenzoates were surveyed in the sequential oxyindation/halogenation process to give 4-halogenated isocoumarins. Substrates with electron withdrawing groups such as nitro and carbonyl groups gave the target products **24b** and **24c** in high yields (entries 3 and 4). The structure of **24b** was characterized by X-ray crystallographic analysis (see Fig. S11† in the ESI). Substrates with methyl or aryl groups efficiently afforded the target isocoumarins **24d** and **24e** (entries 5 and 6). Also, 2-alkynylbenzoates, including halogen moieties (Br, Cl and F), were suitable for this reaction system to give the isocoumarins **25f–24h** in moderate yields (entries 7–9). The synthesis of isocoumarins from internal alkynes was also investigated. The optimization of the reaction conditions showed that gallium salts were more suitable than indium salts for the oxymetalation of an internal alkyne (see Table S3† in the ESI). Therefore, gallium salts were employed in the reactions of internal alkynes **1i–1k** to provide the 3,4-disubstituted isocoumarins **24i**, **24j** and **25k** (entries 10–12).

One-pot syntheses of 4-substituted isocoumarins were performed *via* oxyindation followed by a palladium-catalyzed cross-coupling reaction (Table 3).[30] After the oxymetalation of **1a** using $InBr_3$, the addition of a palladium catalyst, lithium chloride, organic halides **27**, and an additional solvent to the resultant toluene solution afforded the coupling product **28**. Iodobenzene **27a** and aryl iodides bearing an electron donating group **27b** or an electron withdrawing group **27c** were applicable to give the 4-arylisocoumarins **28aa–28ac** in high yields (entry 1). Palladium-catalyzed cross coupling with acid chlorides also proceeded efficiently. Reactions using the benzoyl chloride derivatives **27d** and **27e**, as well as the alkanoyl chloride **27f**, afforded the isocoumarins **28ad–28af** with ketone moieties in good yields (entries 2 and 3). The structure of **28ae** was characterized by X-ray crystallographic analysis (see Fig. S12† in the

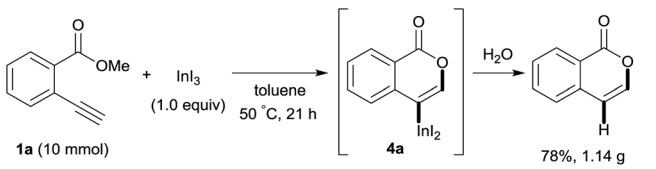

Scheme 7 Gram-scale synthesis of isocoumarin including a carbon–indium bond.

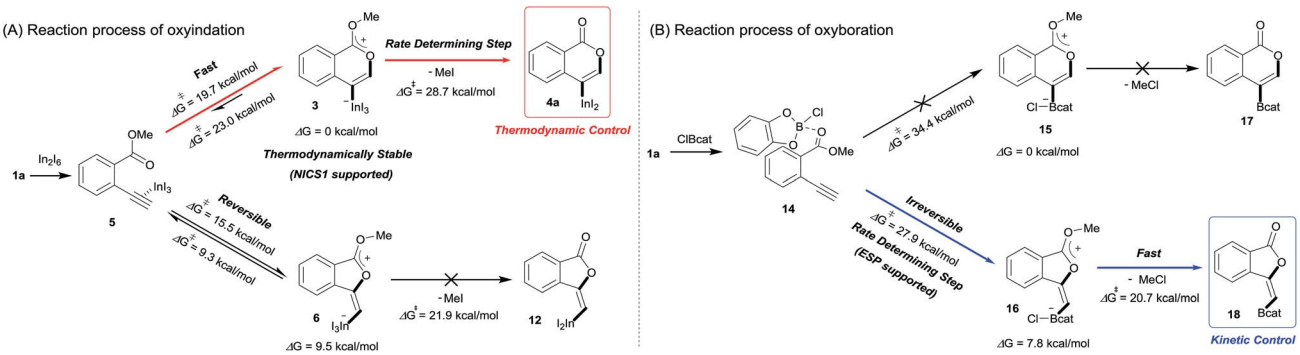

Fig. 8 The summarized results of DFT calculation.

Table 2 Sequential oxymetalation/halogenation of various types of 2-alkynylbenzoate **1**[a]

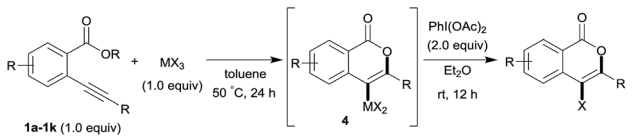

Entry	1	MX_3	Target	Yield[b] (%)
1	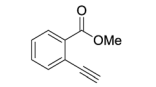 **1a**	InI_3	 **24a**	64
2	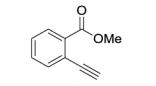 **1a**	$InBr_3$	 **25a**	73
3	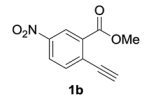 **1b**	InI_3	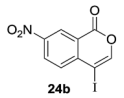 **24b**	61
4	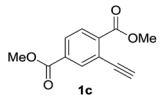 **1c**	InI_3	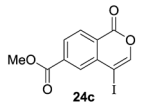 **24c**	70
5	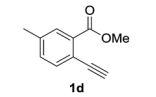 **1d**	InI_3	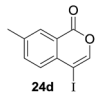 **24d**	54
6	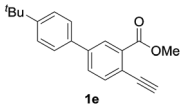 **1e**	InI_3	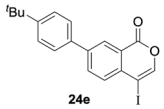 **24e**	54
7	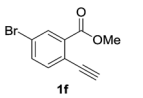 **1f**	$InBr_3$	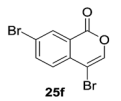 **25f**	47
8	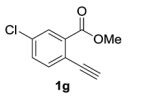 **1g**	InI_3	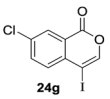 **24g**	67
9	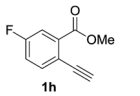 **1h**	InI_3	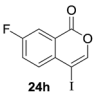 **24h**	61
10	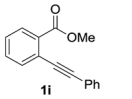 **1i**	GaI_3	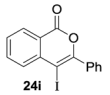 **24i**	60
11	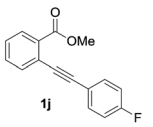 **1j**	GaI_3	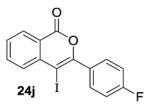 **24j**	56
12	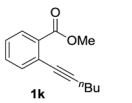 **1k**	$GaBr_3$	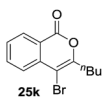 **25k**	60

[a] First step: **1** (0.5 mmol), MX_3 (0.5 mmol), toluene (1 mL), 50 °C, 24 h. Second step: $PhI(OAc)_2$ (1.0 mmol), Et_2O (1 mL), rt, 12 h. [b] Isolated yields.

ESI). In this reaction system, alkyl halides such as benzyl bromide **27g** and allyl bromide **27h** were also suitable to give 4-alkylisocoumarins **28ag** and **28ah**, respectively (entries 4 and 5). Various types of 4-substituted isocoumarins were obtained from an isocoumarin that included a carbon–indium bond by utilizing palladium-catalyzed cross coupling.

Formal total synthesis of oosponol

Finally, a formal total synthesis of oosponol, which exhibits strong antifungal activity,[15] was conducted (Scheme 8). Firstly, the iodination of commercially available compound **29** proceeded *via* a method found in the literature.[31] During the initial investigation, **30** was transformed into methyl 2-ethynyl-6-methoxybenzoate, and then we attempted the synthesis of the precursor of oosponol *via* oxyindation and cross-coupling, but the reaction returned a complicated mixture (see Scheme S1† in the ESI). Therefore, in another synthetic route, the OMe group

Table 3 One-pot formation of 4-substituted isocoumarins by palladium-catalyzed cross coupling of organoindium species **26** with organic halides **27**[a]

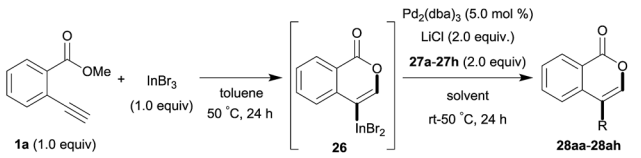

Entry	27	Target	Yield[b] (%)
1	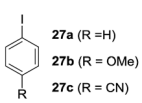 **27a** (R = H) **27b** (R = OMe) **27c** (R = CN)	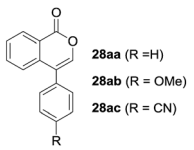 **28aa** (R = H) **28ab** (R = OMe) **28ac** (R = CN)	**28aa:** 81 **28ab:** 71 **28ac:** 72
2	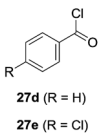 **27d** (R = H) **27e** (R = Cl)	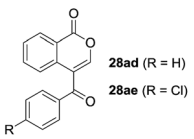 **28ad** (R = H) **28ae** (R = Cl)	**28ad:** 82 **28ae:** 64
3[c]	 **27f**	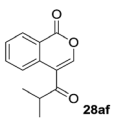 **28af**	61
4[d]	 **27g**	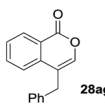 **28ag**	51
5[d]	 **27h**	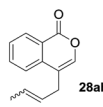 **28ah**	45[e]

[a] Basic reaction conditions of the first step: **1a** (0.5 mmol), $InBr_3$ (0.5 mmol), toluene (1 mL), 50 °C, 24 h. Second step: Pd_2dba_3 (0.025 mmol), LiCl (1.0 mmol), **27** (1.0 mmol), NMP (2.5 mL), 50 °C, 24 h. [b] Isolated yields. [c] HMPA (2.5 mL), rt, 24 h. [d] HMPA (2.5 mL), 50 °C, 24 h. [e] $E/Z = 90:10$.

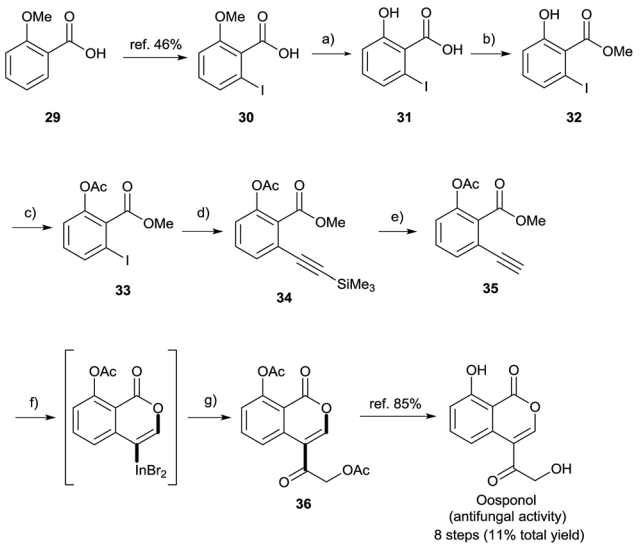

Scheme 8 Formal total synthesis of oosponol. Reagents and reaction conditions: (a) BBr_3 (1 M in CH_2Cl_2, 2.0 equiv.), CH_2Cl_2, rt, 20 h, 100%. (b) H_2SO_4 (20 mol%), MeOH, reflux, 20 h, 87%. (c) AcCl (1.04 equiv.), pyridine (1.04 equiv.), acetone, rt, 14 h, 97%. (d) ethynyltrimethylsilane (1.1 equiv), $PdCl_2(PPh_3)_2$ (2.0 mol%), CuI (20 mol%), NEt_3, RT, 17 h, 100%. (e) 1 M KF aq. (1.65 equiv.), DMF, RT, 0.5 h, 76%. (f) $InBr_3$ (1.0 equiv.), Toluene, 50 °C, 24 h. (g) Pd_2dba_3 (5.0 mol%), LiCl (2.0 equiv.), 2-(acetyloxy)acetyl chloride **27i** (2.0 equiv.), HMPA, rt, 9 h, 44%.

of **29** was converted to an OAc group with less ability to donate electrons. The OMe moiety of **30** was completely deprotected with BBr_3. The acid-catalyzed esterification and acetylation of the phenol moiety gave methyl 6-iodoacetylsalicylate **33** in a high yield. Sonogashira coupling followed by the removal of a silyl moiety afforded the desired 2-alkynylbenzoate derivative **35**. The oxymetalation of **35** using $InBr_3$ and sequential palladium-catalyzed cross coupling with acid chloride **27i** produced the key intermediate **36**, and the hydrolyzation of **36** yielded oosponol.[16b] Our method used a readily available starting material and gave a higher yield than previous studies.[16b,32]

Conclusions

We achieved the synthesis of isocoumarins bearing a metal–carbon bond at the 4-position *via* 6-*endo* selective oxymetalation of 2-alkynylbenzoate **1** (Type *endo*-t). Indium and gallium salts showed high activity for the oxymetalation of 2-ethynylbenzoate **1a**. Both the metalated isocoumarin **4b** and the zwitterion intermediate **3** were identified by X-ray crystallographic analysis. This is the first example of the isolation of the product **E** and the benzopyrylium intermediate **F** proposed in the mechanism of oxymetalation (Scheme 2A). The elimination of MeI from zwitterion **3** occurred under heating conditions to give the target product **4a**, which means that the rate-determining step was the elimination step. DFT calculation suggested that thermodynamic control led to 6-*endo* selective oxyindation, while kinetic control led to 5-*exo* selective oxyboration. The 6-membered product proved much more stable than the 5-membered product due to a difference in the degree of aromatic stability. The investigation of the electrostatic potential of the transition state in the cyclization pathway suggested that a delocalization of negative charge by the large atomic radii of In and I atoms stabilizes the zwitterionic transition state. In contrast, the small atomic radii of B, Cl, and O atoms cause a localization of negative charge to destabilize the corresponding transition state. The difference in stability between the 6- and 5-membered zwitterions and the elemental character of InI_3 both played important roles in the unique regioselectivity of oxymetalation and in the facile preparation of the **E** species.

These isocoumarins bearing a carbon–metal bond at the 4-position were applied to organic synthesis. Oxymetalation provided isocoumarins on a gram scale. The oxidation of organoindium or gallium species yielded various types of 4-halogenated isocoumarins. Palladium-catalyzed cross coupling with aryl iodide, acid chloride, and alkyl bromide gave a wide range of 4-substituted isocoumarins in a one-pot reaction. Therefore, the unprecedented regioselectivity of the present oxymetalation contributed to the synthesis of new types of isocoumarins. We accomplished a formal total synthesis of oosponol to demonstrate the utility of our reaction system.

Conflicts of interest

There are no conflicts to declare.

Acknowledgements

This work was supported by JSPS KAKENHI Grant Numbers JP15H05848 in Middle Molecular Strategy, JP16K05719 and JP18H01977. Y. N. acknowledges support from the Frontier Research Base for Global Young Researchers, Osaka University, of the MEXT program and from Mitsui Chemicals Award in Synthetic Organic Chemistry. We thank Prof. Dr S. Blum (Department of Chemistry, University of California, Irvine) for helpful suggestions. We would like to thank Prof. Dr S. Akai (Graduate School of Pharmaceutical Science, Osaka University, Japan) for suggestions about the total synthesis of oosponol. Thanks are due to the Analytical Instrumentation Facility, Graduate School of Engineering, Osaka University, for assistance in obtaining the MS spectra.

Notes and references

1 (*a*) D. B. Kitchen, H. Decornez, J. R. Furr and J. Bajorath, *Nat. Rev. Drug Discovery*, 2004, **3**, 935–949; (*b*) R. E. Ziegert, J. Toräng, K. Knepper and S. Bräse, *J. Comb. Chem.*, 2005, **7**, 147–169; (*c*) R. A. Ward and J. G. Kettle, *J. Med. Chem.*, 2011, **54**, 4670–4677; (*d*) P. S. Mariano, *Tetrahedron*, 1983, **39**, 3879–3983; (*e*) N. A. Romero and D. A. Nicewicz, *Chem. Rev.*, 2016, **116**, 10075–10166; (*f*) B. H. Lipshutz, *Chem. Rev.*, 1986, **86**, 795–819; (*g*) A. R. Katritzky, *Chem. Rev.*, 1989, **89**, 827–861; (*h*) Y.-G. Zhou, *Acc. Chem. Res.*, 2007, **40**, 1357–1366.

2 (*a*) R. Dorel and A. M. Echavarren, *Chem. Rev.*, 2015, **115**, 9028–9072; (*b*) N. T. Patil and Y. Yamamoto, *Chem. Rev.*, 2008, **108**, 3395–3442; (*c*) F. Alonso, I. P. Beletskaya and

M. Yus, *Chem. Rev.*, 2004, **104**, 3079–3159; (*d*) A. Deiters and S. F. Martin, *Chem. Rev.*, 2004, **104**, 2199–2238; (*e*) V. Nair, C. Rajesh, A. U. Vinod, S. Bindu, A. R. Sreekanth, J. S. Mathen and L. Balagopal, *Acc. Chem. Res.*, 2003, **36**, 899–907.

3 For selective examples:(*a*) J. Liu, X. Xie and Y. Liu, *Chem. Commun.*, 2013, **49**, 11794–11796; (*b*) Y.-J. Feng, F.-Y. Tsai, S.-L. Huang, Y.-H. Liu and Y.-C. Lin, *Eur. J. Inorg. Chem.*, 2014, 5406–5414; (*c*) S. S. Racharlawar, D. Shankar, M. V. Karkhelikar, B. Sridhar and P. R. Likhar, *J. Organomet. Chem.*, 2014, **757**, 14–20; (*d*) J. J. Hirner, D. J. Faizi and S. A. Blum, *J. Am. Chem. Soc.*, 2014, **136**, 4740–4745; (*e*) D. Shankar, K. Jaipal, B. Sridhar, R. N. Chary, S. Prabhakar, L. Giribabu and P. R. Likhar, *RSC Adv.*, 2015, **5**, 20295–20301; (*f*) E. Chong and S. A. Blum, *J. Am. Chem. Soc.*, 2015, **137**, 10144–10147; (*g*) K. N. Tu, J. J. Hirner and S. A. Blum, *Org. Lett.*, 2016, **18**, 480–483; (*h*) D. J. Faizi, N. A. Nava, M. Al-Amin and S. A. Blum, *Org. Synth.*, 2016, **93**, 228–244; (*i*) D. J. Faizi, A. J. Davis, F. B. Meany and S. A. Blum, *Angew. Chem., Int. Ed.*, 2016, **55**, 14286–14290; (*j*) A. J. Warner, A. Churn, J. S. McGough and M. J. Ingleson, *Angew. Chem., Int. Ed.*, 2017, **56**, 354–358; (*k*) N. Chaisan, W. Kaewsri, C. Thongsornkleeb, J. Tummatorn and S. Ruchirawat, *Tetrahedron Lett.*, 2018, **59**, 675–680.

4 (*a*) Y. Kato, K. Miki, F. Nishino, K. Ohe and S. Uemura, *Org. Lett.*, 2003, **5**, 2619–2621; (*b*) C. P. Casey, N. A. Strotman and I. A. Guzei, *Organometallics*, 2004, **23**, 4121–4130; (*c*) R. Vicente, J. González, L. Riesgo, J. González and L. A. López, *Angew. Chem., Int. Ed.*, 2012, **51**, 8063–8067; (*d*) T. Murata, M. Murai, Y. Ikeda, K. Miki and K. Ohe, *Org. Lett.*, 2012, **14**, 2296–2299; (*e*) Y. Xia, S. Qu, Q. Xiao, Z.-X. Wang, P. Qu, L. Chen, Z. Liu, L. Tian, Z. Huang, Y. Zhang and J. Wang, *J. Am. Chem. Soc.*, 2013, **135**, 13502–13511; (*f*) J.-M. Yang, Z.-Q. Li, M.-L. Li, Q. He, S.-F. Zhu and Q.-L. Zhou, *J. Am. Chem. Soc.*, 2017, **139**, 3784–3789.

5 (*a*) K. Miki, T. Yokoi, F. Nishino, K. Ohe and S. Uemura, *J. Organomet. Chem.*, 2002, **645**, 228–234; (*b*) K. Miki, T. Yokoi, F. Nishino, Y. Kato, Y. Washitake, K. Ohe and S. Uemura, *J. Org. Chem.*, 2004, **69**, 1557–1564; (*c*) K. Okamoto, M. Watanabe, A. Mashida, K. Miki and K. Ohe, *Synlett*, 2013, **24**, 1541–1544.

6 (*a*) R. C. Larock and L. W. Harrison, *J. Am. Chem. Soc.*, 1984, **106**, 4218–4227; (*b*) A. Nagarajan and T. R. Balasubramanian, *Indian J. Chem., Sect. B: Org. Chem. Incl. Med. Chem.*, 1987, **26B**, 917–919; (*c*) Y. Zhu and B. Yu, *Angew. Chem., Int. Ed.*, 2011, **50**, 8329–8332; (*d*) Y. Tang, J. Li, Y. Zhu, Y. Li and B. Yu, *J. Am. Chem. Soc.*, 2013, **135**, 18396–18405; (*e*) D. J. Faizi, A. Issaian, A. J. Davis and S. A. Blum, *J. Am. Chem. Soc.*, 2016, **138**, 2126–2129; (*f*) B. Akkachairin, J. Tummatorn, N. Supantanapong, P. Nimnual, C. Thongsornkleeb and S. Ruchirawat, *J. Org. Chem.*, 2017, **82**, 3727–3740.

7 The metal species **E** was proposed as intermediate for oxymetalation/protonation sequential reactions, and these cyclic reactions showed low regioselectivity to afford mixture of 5- and 6-membered rings.(*a*) E. Marchal, P. Uriac, B. Legouin, L. Toupet and P. v. d. Weghe, *Tetrahedron*, 2007, **63**, 9979–9990; (*b*) B. Y.-W. Man, A. Knuhtsen, M. J. Page and B. A. Messerle, *Polyhedron*, 2013, **61**, 248–252.

8 (*a*) I. V. Alabugin, K. Gilmore and M. Manoharan, *J. Am. Chem. Soc.*, 2011, **133**, 12608–12623; (*b*) K. Gilmore, R. K. Mohamed and I. V. Alabugin, *WIREs Comput. Mol. Sci.*, 2016, **6**, 487–514.

9 (*a*) I. V. Alabugin and K. Gilmore, *Chem. Commun.*, 2013, **49**, 11246–11250; (*b*) P. W. Peterson, R. K. Mohamed and I. V. Alabugin, *Eur. J. Org. Chem.*, 2013, 2505–2527; (*c*) T. Yao and R. C. Larock, *J. Org. Chem.*, 2003, **68**, 5936–5942.

10 Although some groups reported 6-endo cyclic oxymetalation using terminal alkynes, the formed 6-membered pyrylium intermediate **F** was trapped by a nucleophile to give not **E** but heterocyclic compounds or naphthalene derivatives, and **F** has not been isolated.(*a*) N. Iwasawa, M. Shido and H. Kusama, *J. Am. Chem. Soc.*, 2001, **123**, 5814–5815; (*b*) N. Asao, T. Nogami, K. Takahashi and Y. Yamamoto, *J. Am. Chem. Soc.*, 2002, **124**, 764–765; (*c*) H. Kusama, H. Funami, J. Takaya and N. Iwasawa, *Org. Lett.*, 2004, **6**, 605–608; (*d*) N. T. Patil and Y. Yamamoto, *J. Org. Chem.*, 2004, **69**, 5139–5142; (*e*) H. Kusama, H. Funami, M. Shido, Y. Hara, J. Takaya and N. Iwasawa, *J. Am. Chem. Soc.*, 2005, **127**, 2709–2716; (*f*) H. Kusama, H. Funami and N. Iwasawa, *Synthesis*, 2007, 2014–2024; (*g*) R. Yanada, K. Hashimoto, R. Tokizane, Y. Miwa, H. Minami, K. Yanada, M. Ishikura and T. Takemoto, *J. Org. Chem.*, 2008, **73**, 5135–5138; (*h*) X.-L. Fang, R.-Y. Tang, X.-G. Zhang, P. Zhong, C.-L. Deng and J.-H. Li, *J. Organomet. Chem.*, 2011, **696**, 352–356; (*i*) S. Zhu, Z. Zhang, X. Huang, H. Jiang and Z. Guo, *Chem.–Eur. J.*, 2013, **19**, 4695–4700; (*j*) G. Mariaule, G. Newsome, R. Y. Toullec, P. Belmont and V. Michelet, *Org. Lett.*, 2014, **16**, 4570–4573; (*k*) J.-F. Cui, H.-M. Ko, K.-P. Shing, J.-R. Deng, N. C.-H. Lai and M.-K. Wong, *Angew. Chem., Int. Ed.*, 2017, **56**, 3074–3079.

11 (*a*) R. D. Barry, *Chem. Rev.*, 1964, **64**, 229–260; (*b*) R. A. Hill, in *Progress in the Chemistry of Organic Natural Products*, ed. W. Herz, 1986, vol. 49, pp. 1–78; (*c*) I.-U. Rahman, M. Arfan and G. A. Khan, *J. Chem. Soc. Pak.*, 1998, **20**, 76–87; (*d*) V. Rukachaisirikul, A. Rodglin, Y. Sukpondma, S. Phongpaichit, J. Buatong and J. Sakayaroj, *J. Nat. Prod.*, 2012, **75**, 853–858; (*e*) M. E. Riveiro, A. Moglioni, R. Vazquez, N. Gomez, G. Facorro, L. Piehl, E. R. De Celis, C. Shayo and C. Davio, *Bioorg. Med. Chem.*, 2008, **16**, 2665–2675; (*f*) L. M. Bedoya, E. Del Olmo, R. Sancho, B. Barboza, M. Beltrán, A. E. García-Cadenas, S. Sánchez-Palomino, J. L. López-Pérez, E. Muñoz, A. S. Feliciano and J. Alcamí, *Bioorg. Med. Chem. Lett.*, 2006, **16**, 4075–4079; (*g*) N. Agata, H. Nogi, M. Milhollen, S. Kharbanda and D. Kufe, *Cancer Res.*, 2004, **64**, 8512–8516; (*h*) T. Nakashima, S. Hirano, N. Agata, H. Kumagai, K. Isshiki, T. Yoshioka, M. Ishizuka, K. Maeda and T. Takeuchi, *J. Antibiot.*, 1999, **52**, 426–428; (*i*) M. Yoshikawa, E. Harada, Y. Noritoh, K. Inoue, H. Matsuda, H. Shimoda, J. Yamahara and N. Murakami, *Chem. Pharm. Bull.*, 1994, **42**, 2225–2230; (*j*) T. Furuta,

Y. Fukuyama and Y. Asakawa, *Phytochemistry*, 1986, **25**, 517–520.

12 (*a*) N. Panda, P. Mishra and I. Mattan, *J. Org. Chem.*, 2016, **81**, 1047–1056; (*b*) K. Kobayashi, W. Miyatani and M. Kuroda, *Helv. Chim. Acta*, 2013, **96**, 2173–2178; (*c*) M. Lessi, T. Masini, L. Nucara, F. Bellina and R. Rossi, *Adv. Synth. Catal.*, 2011, **353**, 501–507; (*d*) M. P. Pavan, M. Chakravarty and K. C. K. Swamy, *Eur. J. Org. Chem.*, 2009, 5927–5940; (*e*) Z. He and A. K. Yudin, *Org. Lett.*, 2006, **8**, 5829–5832; (*f*) M. Chakravarty and K. C. K. Swamy, *J. Org. Chem.*, 2006, **71**, 9128–9138; (*g*) S. Kim, G.-J. Fan, J. Lee, J. J. Lee and D. Kim, *J. Org. Chem.*, 2002, **67**, 3127–3130; (*h*) B. A. Kowalczyk, *Synthesis*, 2000, 1113–1116; (*i*) P. Babin and J. Dunoguès, *Tetrahedron Lett.*, 1984, **25**, 4389–4392; (*j*) K. Beautement and J. M. Clough, *Tetrahedron Lett.*, 1984, **25**, 3025–3028; (*k*) O. S. Wolfbeis, *Liebigs Ann. Chem.*, 1981, 819–827.

13 M. Kimura, I. Waki and M. Kokubo, *Jpn. J. Pharmacol.*, 1978, **28**, 693–697.

14 J. H. Lee, Y. J. Park, H. S. Kim, Y. S. Hong, K.-W. Kim and J. J. Lee, *J. Antibiot.*, 2001, **54**, 463–466.

15 (*a*) J. Sonnenbichler and T. Kovács, *Eur. J. Biochem.*, 1997, **246**, 45–49; (*b*) T. Kovács and J. Sonnenbichler, *Liebigs Ann./Recl.*, 1997, **1**, 211–212; (*c*) K. Nozawa, M. Yamada, Y. Tsuda, K. Kawai and S. Nakajima, *Chem. Pharm. Bull.*, 1981, **29**, 2689–2691.

16 (*a*) S. Nakajima, K. Kawai and S. Yamada, *Phytochemistry*, 1976, **15**, 327; (*b*) T. Kovács, I. Sonnenbichler and J. Sonnenbichler, *Liebigs Ann./Recl.*, 1997, **4**, 773–777.

17 (*a*) Y. Nishimoto, H. Ueda, M. Yasuda and A. Baba, *Chem.–Eur. J.*, 2011, **17**, 11135–11138; (*b*) Y. Nishimoto, R. Moritoh, M. Yasuda and A. Baba, *Angew. Chem., Int. Ed.*, 2009, **48**, 4577–4580.

18 For selective examples:(*a*) H. Wang, Y. Kuang and J. Wu, *Asian J. Org. Chem.*, 2012, **1**, 302–312; (*b*) E. Tomás-Mendivil, F. C. Heinrich, J.-C. Ortuno, J. Starck and V. Michelet, *ACS Catal.*, 2017, **7**, 380–387.

19 Benzopyrylium intermediate in oxymetalation was detected by NMR studies or MS sepctra:(*a*) Y. Zhu and B. Yu, *Chem.–Eur. J.*, 2015, **21**, 8771–8780; (*b*) B. N. Nguyen, L. A. Adrin, E. M. Barreiro, J. B. Brazier, P. Haycock, K. K. Hii, M. Nachtegaal, M. A. Newton and J. Szlachetko, *Organometallics*, 2012, **31**, 2395–2402Other types of zwitterion intermediate have been characterized by X-ray crystallographic analysis:(*c*) O. A. Egorova, H. Seo, Y. Kim, D. Moon, Y. M. Rhee and K. H. Ahn, *Angew. Chem., Int. Ed.*, 2011, **50**, 11446–11450; (*d*) Y. Yu, G. Chen, L. Zhu, Y. Liao, Y. Wu and X. Huang, *J. Org. Chem.*, 2016, **81**, 8142–8154.

20 I. Braun, A. M. Asiri and A. S. K. Hashmi, *ACS Catal.*, 2013, **3**, 1902–1907.

21 T. M. Baber, G. Qadeer, G. S. Khan, N. H. Rama and W.-Y. Wong, *Acta Crystallogr.*, 2006, **62**, o5612–o5613.

22 J. D. Forrester, A. Zalkin and D. H. Templeton, *Inorg. Chem.*, 1964, **3**, 63–67.

23 S_N2-type elimination of MeI agrees with the inhibition of the elimination step by bulky *O*-alkyl group in ester moiety (see Table S1† in ESI).

24 The values of the activation energy of the cyclization step shown in Fig. 3 (6-*endo*: 39.4 kcal mol^{-1}, 5-*exo*: 31.0 kcal mol^{-1}) are equivalent to two molecules. The activation energy, which is equivalent to one molecule, is a half of the values (6-*endo*: 19.7 kcal mol^{-1}, 5-*exo*: 15.5 kcal mol^{-1}).

25 (*a*) A. R. Katritzky, *Chem. Rev.*, 2001, **101**, 1421–1449; (*b*) P. v. R. Schleyer, C. Maerker, A. Dransfeld, H. Jiao and N. J. R. v. E. Hommes, *J. Am. Chem. Soc.*, 1996, **118**, 6317–6318.

26 (*a*) A. Issaian, D. J. Faizi, J. O. Bailey, P. Mayer, G. Berionni, D. A. Singleton and S. A. Blum, *J. Org. Chem.*, 2017, **82**, 8165–8178; (*b*) J. Jiang, Z. Zhang and Y. Fu, *Asian J. Org. Chem.*, 2017, **6**, 282–289.

27 X. Shi, N. El Hassan, A. Ikni, W. Li, N. Guiblin, A. Spasojević de-Biré and N. E. Ghermani, *CrystEngComm*, 2016, **18**, 3289–3299.

28 P. Schwerdtfeger, Atomic Static Dipole Polarizabilities, in *Atoms, Molecules and Clusters in Electric Fields*, ed. G. Maroulis, Imperial College Press, London, 2006, pp. 1–32.

29 Silyl anion is stable than carboanion because of the larger atomic radius and higher dipole polarizability of silicon. A. C. Hopkinson and M. H. Lien, *Tetrahedron*, 1981, **37**, 1105–1112.

30 K. Zhao, L. Shen, Z.-L. Shen and T.-P. Loh, *Chem. Soc. Rev.*, 2017, **46**, 586–602.

31 T.-H. Nguyen, A.-S. Castanet and J. Mortier, *Org. Lett.*, 2006, **8**, 765–768.

32 M. Uemura and T. Sakan, *J. Chem. Soc. D*, 1971, **16**, 921.

